Environmental Research 269 (2025) 120911

Contents lists available at ScienceDirect

Environmental Research

journal homepage: www.elsevier.com/locate/envres

Magnetic and reusable Fe_3O_4/PPE-2 functional material for efficient photodegradation of organic dye

Davronbek Bekchanov [a,*], Mukhtarjan Mukhamediev [a], Arofat Inkhonova [a], Davron Eshtursunov [a], Gulbakhor Babojonova [b], Otamurot Rajabov [c], Umedjon Khalilov [c], Maksudbek Yusupov [c], Peter Lieberzeit [d]

[a] Department of Polymer Chemistry, Faculty of Chemistry, National University of Uzbekistan, Tashkent, Uzbekistan
[b] Department of Pharmaceutical and Chemistry, Alfraganus University, Tashkent, Uzbekistan
[c] Arifov Institute of Ion-Plasma and Laser Technologies, Uzbekistan Academy of Sciences, Tashkent, Uzbekistan
[d] Faculty for Chemistry, Department of Physical Chemistry, University of Vienna, Vienna, Austria

ARTICLE INFO

Keywords:
Magnetite
Anion exchange material
PPE-2
Photocatalyst
Hydrothermal
Nanoparticles
Dye degradation

ABSTRACT

Composite photocatalysts based on metal nanoparticles and functional polymers attract much attention compared to inorganic photocatalysts. In this study, a reusable magnetite/anion exchanger (Fe_3O_4/PPE-2) functional material is synthesized by a hydrothermal method, and its photocatalytic activity is evaluated for the photocatalytic degradation of Rhodamine B (RhB). The results from materials characterization confirm a well-defined morphology of magnetic Fe_3O_4/PPE-2 functional material and the formation of Fe_3O_4 nanocrystals with different shapes and sizes on the surface of anion exchange material (PPE-2). The optimized Fe_3O_4/PPE-2 in 180 °C (FM180) photocatalyst exhibited a band gap energy of 1.90 eV, demonstrating significant photocatalytic potential. Using RhB as a model pollutant, magnetic Fe_3O_4/PPE-2 (FM180) functional material achieved 98.2% degradation efficiency after 160 min of visible light irradiation (rate constant k = 0.03496 min^{-1}). Efficiency of the photocatalytic materials, of photocatalytic degradation of RhB is 28.4% for pure anion exchanger (PPE-2), 56.5%, 64.7% and 98.2% for magnetic functional Fe_3O_4/PPE-2 materials, synthesized under conditions of 140 °C (FM140), 160 °C (FM160) and 180 °C (FM180), respectively. Compared to individual PPE-2 anion exchange material and Fe_3O_4, the magnetic functional FM180 material exhibits a remarkable photocatalytic reaction rate as high as four times that of PPE-2, with superior reusability over 10 cycles. The computational study and Mott-Schottky plots verify the formation of the internal electric field. Possible reaction pathways for the photocatalytic degradation of RhB are presented. In addition, the results demonstrate that the Fe_3O_4/PPE-2 functional material very efficiently removed Rhodamine B from textile wastewater. This work offers a simple route for the preparation of magnetic and reusable Fe_3O_4/PPE-2 magnetic functional material that can be used in the water purification process.

1. Introduction

The presence of synthetic organic dyes in textile wastewater significantly contributes to environmental pollution, posing serious risks due to their toxicity and potential carcinogenic effects on aquatic ecosystems and human health (Dutta et al., 2024). Traditional wastewater treatment methods such as filtration, electrochemical degradation, coagulation, ozonation and adsorption are often unable to completely remove persistent pollutants (Kato and Kansha, 2024). Among the advanced environmental remediation technologies, photocatalysis has attracted the attention of industry experts worldwide due to its ability to effectively decompose and mineralize various pollutants in wastewater. Photocatalysis is used as the most effective, harmless and environmentally friendly method for treating textile wastewater (Iqbal et al., 2024). This method involves the activation of semiconductor nanomaterials by light irradiation, resulting in the formation of highly reactive radicals that participate in oxidation-reduction reactions with target pollutants.

In recent years, functional materials, containing iron oxide nanoparticles, with magnetic properties have been widely used in various fields (Ghosh et al., 2020; Vargas-Ortiz et al., 2022). Functional

* Corresponding author.
E-mail address: bekchanovdj@gmail.com (D. Bekchanov).

https://doi.org/10.1016/j.envres.2025.120911
Received 8 November 2024; Received in revised form 31 December 2024; Accepted 19 January 2025
Available online 22 January 2025

materials obtained by incorporating magnetite nanoparticles (Fe_3O_4 NPs) into organic and inorganic polymer matrices are applied in various areas of application, such as separation technology (Qiao et al., 2017), protein immobilization (Xu et al., 2009), catalysis and photocatalysis (Zhu et al., 2013), medical science (Ulbrich et al., 2016), environment (Tan et al., 2013), etc. The polymer macromolecule improves the stability of Fe_3O_4 NPs immobilized in the matrix and increases its functionality (catalytic, sorption, magnetic, etc.) (Iconaru et al., 2016a). The properties of functional materials containing Fe_3O_4 NPs can vary depending on nanoparticle size and shape (Nguyen et al., 2021a).

In general, Fe_3O_4 NPs are agglomerated under the influence of magnetic force and van der Waals force. To reduce this phenomenon and increase the stability of Fe_3O_4 NPs, polymer functionalization is performed on the surface of magnetic nanoparticles. For this, physical and chemical methods are used to form Fe_3O_4 NPs with magnetic properties on the surface of polymer macromolecules (Ma et al., 2019). Certainly, to obtain functional materials with magnetic properties, Fe_3O_4 NPs are synthesized by impregnating the polymer matrix in the synthesis solution using various methods, such as hydrothermal, co-precipitation, sol-gel, microemulsion, etc. (Iconaru et al., 2016b; Qiao and Swihart, 2017; Simeonidis et al., 2007; Fried et al., 2001; Xu et al., 2007; Kang et al., 1996; Ghanbari et al., 2014). Silva et al. (2013) used a co-precipitation method to synthesize Fe_3O_4 NPs on the surface of a polymer macromolecule. For this, the polysaccharide macromolecule was coated with Fe_3O_4 NPs by co-precipitation of Fe^{2+} and Fe^{3+} on the surface of fucan polysaccharides. Chen et al. (2020) synthesized a magnetic functional nanocomposite material. For this functional material, magnetic/carboxymethyl cellulose (Fe_3O_4/CMC) was first prepared by a co-precipitation method, and then, it was combined with functional graphene oxide (GO) to obtain the Fe_3O_4/CMC-supported GO composite (Fe_3O_4/CMC/GO), which exhibited a high sorption capacity for Cu (II) ions. Also, Zhang et al. (2019) used the co-precipitation method to immobilize magnetite NPs on the polymer surface grafted with poly (dopamine)(3-aminopropyl)triethoxysilane for obtaining a surface functionalized material containing Fe_3O_4 NPs. Functional materials containing Fe_3O_4 NPs are used in wastewater treatment by efficient photocatalytic degradation of organic dyes (Matar and Andac, 2024), antibiotics (Zulfiqar et al., 2024), phenol derivatives (Ur Rehman et al., 2019), etc. Toxic organic compounds have a negative effect on flora, fauna, and other living organisms present in water. Especially, wastewater from textile industries is highly contaminated with toxic organic dyes (Al-Tohamy et al., 2022). Using a sorption method for the removal of toxic organic dyes from contaminated water is inefficient. One of the effective methods for wastewater treatment from toxic organic dyes is photocatalysis (Kumari et al., 2023). Previous studies (Madima et al., 2022; Bilgic, 2022; Manohar et al., 2021; Esbergenova et al., 2024) used various functional materials with magnetic properties containing Fe_3O_4 NPs, in comparison to other photocatalysts, because of the possibility of multiple reuses in wastewater treatment. However, functional materials obtained by a surface modification of inorganic materials with Fe_3O_4 NPs have limited properties. This necessitates applying other methods for obtaining the surface-functionalized materials with the presence of Fe_3O_4 NPs on the surface of other functional organic polymer materials. For instance, obtaining surface-functionalized photocatalytic materials by the immobilization of MeO NPs under hydrothermal conditions into ion exchange materials based on organic polymers is widely used. Since functional polymers in the MeO/polymer composites stabilize MeO NPs and increase their charge transfer and reusability, functional polymers have a positive effect on photocatalytic efficiency.

Currently, wastewater from textile factories is purified using the sorbents in the sorption process. However, this method of purification turned out to be ineffective, and on the other hand, after sorption, it is necessary to regenerate the sorbent for reuse. Though, after desorption of sorbed dyes, it is impossible to utilize. The main novelty and importance of this work was the effective purification of textile wastewater from organic dye Rhodamine B using photocatalytic functional Fe_3O_4/PPE-2 material based on $FeCl_2 \bullet 4H_2O$, $FeCl_3 \bullet 6H_2O$ and anion exchanger PPE-2. The structural and morphological properties of the synthesized functional Fe_3O_4/PPE-2 materials were characterized using various techniques. The Fe_3O_4/PPE-2 functional material synthesized at 180 °C (FM180) exhibited a narrower bandgap 1.90 eV compared to those synthesized at 140 °C and 160 °C (FM140 and FM160) 2.10 eV and1.92 eV respectively. This narrower bandgap enables FM180 to absorb more light from the visible-light region contributing to the generation of more charge carriers. The functional FM180 material exhibited enhanced photocatalytic degradation of Rhodamine B under visible light irradiation compared to pristine PPE-2 also functional FM140 and FM160 materials. Using the synthesized Fe_3O_4/PPE-2 functional materials, highly efficient purification of textile wastewater from the toxic organic dye Rhodamine B was carried out in photocatalytic degradation at a temperature of 308 K in a neutral environment (pH 6.5) solution. The purification of textile wastewater from Rhodamin B was carried out cyclically, and the wastewater purification efficiency of the Fe_3O_4/PPE-2 functional material was after ten cycles not less than 94.4%.

2. Experimental

2.1. Materials

The synthesis of the anion exchange material (PPE-2) required the use of granular polyvinylchloride and urea (Bekchanov et al., 2023). Granular polyvinylchloride (70%, JSC "NAVOIAZOT", Uzbekistan) and urea (97%, JSC "NAVOIAZOT", Uzbekistan). Fe_3O_4 NPs were synthesized using $FeCl_3 \cdot 6H_2O$ (98%, Sigma-Aldrich) and $FeSO_4 \cdot 7H_2O$ (98%, Sigma-Aldrich). Additional reagents employed in this study included NH_4OH (25%, Sigma-Aldrich), Rhodamine B (98%, Sigma-Aldrich), ethanol (96%, Sigma-Aldrich), and ethyl acetate (99%, Sigma-Aldrich). Commercially available deionized water was used throughout the experiments.

2.2. Synthesis of PPE-2

The anion exchanger (PPE-2) was synthesized based on the methods described in previous articles with modifications of granulated polyvinyl chloride (Bekchanov et al., 2023). To synthesize PPE-2, 5 g of granulated plasticized polyvinyl chloride and 10 g of urea ($H_2N\text{-}CO\text{-}NH_2$) were mixed for 8 h at a temperature of 423 K. The modification process was carried out in a Teflon-lined autoclave in a double convection oven (DOF-H series) to heat the reaction mixture. During the modification of polyvinyl chloride with urea, the Cl atoms in the macromolecule interact with the amino groups of urea. As a result, the amino groups are attached to the macromolecule. After modification, the resulting anion exchanger PPE-2 was washed and activated using HCl and NaOH solutions. Scheme 1 shows the reaction of PPE-2 synthesis.

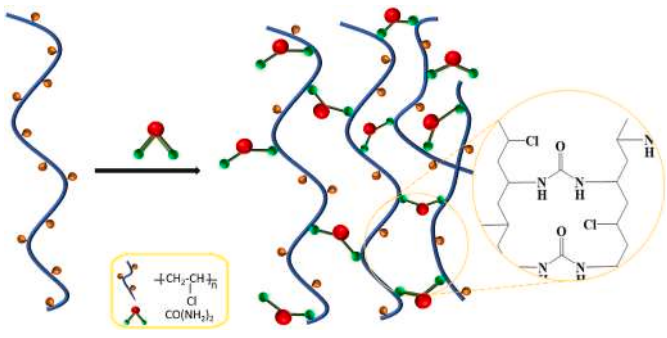

Sheme 1. Reaction scheme of modification of the PVC with urea.

2.3. Preparation of Fe_3O_4/PPE-2 functional material

Anion exchange material (PPE-2, 2 g) was introduced into a 250-mL three-neck round-bottomed flask, and 50 mL of deionized water was added. The mixture was heated to 60 °C, with stirring at 400 rpm, for 15 min to obtain a homogeneous dispersion. Then, 0.88 g of $FeCl_2{\cdot}4H_2O$ and 0.6 g of $FeCl_3{\cdot}6H_2O$ were simultaneously introduced into the above suspension containing PPE-2, and the nitrogen gas was purged until a full dissolution of iron salts. For the synthesis of Fe_3O_4/PPE-2 functional material, the initial reagents $FeCl_2{\bullet}4H_2O$, $FeCl_3{\bullet}6H_2O$ and PPE-2 anion exchanger were taken in mass ratios of 0.44:0.3:1, respectively. About 20 mL of $NH_3{\cdot}H_2O$ was added to the solution to adjust its pH to 10.0–11.0, and black nanoparticles were precipitated after 10 min. The suspension was subjected to hydrothermal treatment under different temperatures and times: (i) 140 °C for 2 h, (ii) 160 °C for 4 h, and (iii) 180 °C for 6 h. The samples were labeled as FM140, FM160, and FM180 according to their synthesis temperatures. The photocatalytic properties of the samples did not change when the synthesis time of FM140, FM160, and FM180 samples was increased. After the hydrothermal treatment, the samples were collected using a magnet, washed with deionized water several times, and dried at 50 °C for 24 h. Fig. 1 shows a schematic representation of the synthesis of magnetic Fe_3O_4/PPE-2 functional material.

2.4. Characterization

The crystalline phases of the synthesized magnetic functional material were analyzed using an X-ray diffractometer (XRD, D8 Advance, Bruker). Based on the results of X-ray diffraction analysis of FM140, FM160, and FM180 samples, the crystal size on the surface of the samples was theoretically determined using the Scherrer equation (Eq. (1)).The microstructures of the synthesized magnetic functional material were observed using an EVO MA-10 scanning electron microscope (SEM, Carl Zeiss). The chemical composition of the synthesized magnetic functional material was analyzed by an energy-dispersive X-ray microanalysis system (Oxford Instruments), attached to the scanning electron microscope. Fourier-transform infrared (FTIR) spectrometer (Spectrum100, PerkinElmer), equipped with an FTIR microscopy accessory, on the attenuated total reflection (ATR) diamond crystal was used at room temperature over a frequency of 500–4000 cm^{-1}. With AutosorbiQ, Quantachrome, USA, nitrogen (N_2) adsorption-desorption isotherms were measured at 77 K to calculate the average pore size distributions and pore volumes for Barrett-Joyner Halenda (BJH) and Brunauer-Emmett-Teller (BET) specified surface areas. At normal temperature, the materials photoluminescence (PL) spectrum was measured using a Cary Eclipse Fluorescence Spectrophotometer (Agilent Technologies) Light Source Xenon flash lamp (80 Hz). The ultraviolet–visible (UV–Vis) diffuse reflectance spectra of the synthesized magnetic functional material were measured on a UV–Vis–NIR spectrophotometer (UV-3600, Shimadzu).

$$D = \frac{K\lambda}{\beta \bullet Cos\,\theta} \tag{1}$$

where D – average crystallite size (in nanometers, nm), K – Scherrer constant (typically around 0.94), λ – wavelength of X-ray radiation used (in angstroms, Á = 1.5406), β – full width at half maximum (FWHM) of the diffraction peak (in radians), θ – diffraction (Bragg) angle (in radians).

2.5. Photocatalytic activity tests

The photocatalytic activities of the synthesized magnetic functional materials were evaluated by degrading Rhodamine B (50 mg L^{-1}) in a JT-GHX-AC photocatalytic reactor using UV light irradiation (300 W, λ = 254 nm). Typically, the sample (50 mg) was dispersed in 50 mL Rhodamine B aqueous solution for 30 min in the dark to reach adsorption-desorption equilibrium. Afterward, the RhB-containing suspension was irradiated by UV light. The samples were collected, filtered, and analyzed using a UV-i1900 spectrophotometer (Shimadzu). To calculate the photocatalytic degradation efficiency (E) of Rhodamine B, Eq. (2) was used:

$$E\% = \frac{C_0 - C_t}{C_0} \times 100, \tag{2}$$

where C_0 and C_t are the concentrations of Rhodamine B (mg/L) at the initial and at the time, respectively. The kinetics of the photocatalytic degradation process of Rhodamine B was studied using the first-order kinetic model (Eq. (3)) in accordance with the Langmuir-Hinshelwood kinetic model:

$$ln\frac{C_0}{C_t} = kt, \tag{3}$$

where k and t are the kinetic rate constant and irradiation time, respectively. The k value indicates the photocatalytic activity and the linear plot slope calculated it. Additionally, the reusability test for the best-performing functional material was conducted over 10 cycles under the same conditions. The mixture of ethanol and deionized water was used to wash the collected sample after each cycle and dried at 50 °C for 24 h.

3. Results and DISCUSSION

3.1. Characterizations of photocatalysts

By changing the hydrothermal synthesis temperature, Fe_3O_4 nanoparticles were formed on the surface of PPE-2 anion exchange material. The XRD patterns of the samples hydrothermally treated at 140 °C (sample FM140), 160 °C (sample FM160), and 180 °C (sample FM180) are shown in Fig. 2 along with the XRD pattern of anion exchange material (PPE-2). In Fig. 2a, the XRD pattern of PPE-2 has a broad halo reflection at $2\theta = 25°$, indicating its amorphous nature. A weak reflection in the range of $2\theta = 40°$–$45°$ is the indication of a partially carbonized polymer.

Fig. 2b presents the XRD patterns of the FM140 sample, which display multiple reflection peaks within the diffraction range of 20–90°.

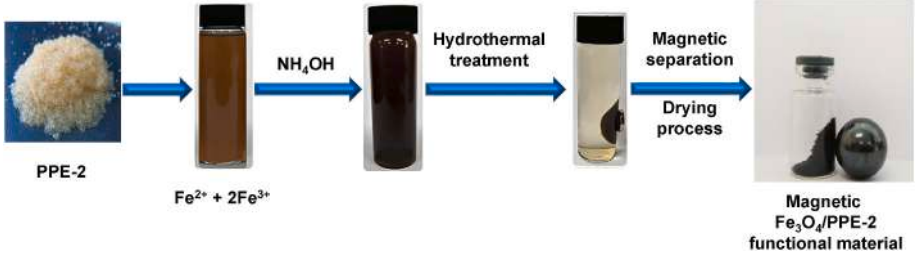

Fig. 1. Schematic representation of the synthesis of magnetic Fe_3O_4/PPE-2 functional material.

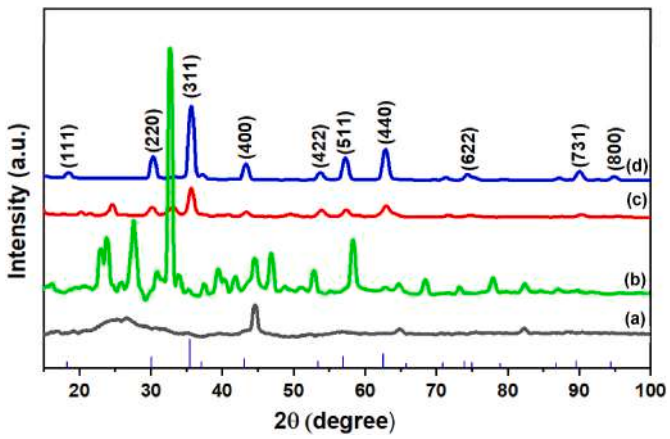

Fig. 2. XRD patterns of PPE-2 (a) and magnetic Fe_3O_4/PPE-2 functional material synthesized at different temperatures and times: (b) FM140, (c) FM160, and (d) FM180.

Notably, the peaks at 2θ = 27.25°, 45.25°, and 57.28° correspond well to the crystallographic planes (220), (311), and (511) of Fe_3O_4, respectively (JCPDS85-1436 for Fe_3O_4). These peaks are primarily observed after heating the sample to 140 °C, indicating the initial formation of partially spherical Fe_3O_4 nanocrystals on the surface of the PPE-2 anion exchange material. Additionally, the XRD pattern shows peaks at 2θ = 23.78°, 32.6°, and 64.64°, corresponding to the (012), (104), and (300) planes, respectively, which are characteristic of Fe_2O_3 crystals (JCPDS 33–0664). The presence of mixed phases of Fe_2O_3 and Fe_3O_4 under the given synthesis conditions indicates the formation of iron oxide crystals and suggests an ongoing transition from Fe_2O_3 to Fe_3O_4 phases. In the case of sample FM160 (Fig. 2c), the reflections in the XRD pattern can be observed at 2θ = 30.3°, 35.6°, 43.28°, 53.6°, 57.18°, and 62.8°, which can be assigned to the (220), (311), (400), (422), (511), and (440) crystallographic planes of Fe_3O_4. In the XRD pattern of FM180 in Fig. 2d, the characteristic reflections observed at 2θ = 18.51°, 30.32°, 35.66°, 43.32°, 53.75°, 57.26°, 62.86°, 74.31°, 90.06°, and 94.9° correspond to the (111), (220), (311), (400), (422), (511), (400), (622), (731), and (800) crystallographic (JCPDS 85–1436) planes of Fe_3O_4 synthesized and immobilized on the surface of PPE-2 (Nguyen et al., 2021b). During the formation of Fe_3O_4 nanoparticles on the surface of PPE-2, the size and morphology of Fe_3O_4 nanocrystals are expected to vary because of synthesis temperature and time. The average sizes of Fe_3O_4 nanocrystals, estimated using Scherrer's equation (Eq. (1)), were found to be 48, 38, and 18 nm for FM140, FM160, and FM180 samples, respectively. No reflections assignable to the foreign crystalline phases were detected, suggesting favorable conditions for the synthesis of magnetic Fe_3O_4/PPE-2 functional material.

The microstructures of magnetic Fe_3O_4/PPE-2 functional material was examined by scanning electron microscopy (SEM). The SEM images of FM140, FM160, and FM180 samples are shown in Fig. 3. As can be seen in Fig. 3a, spherical nanocrystals of Fe_3O_4 were formed on the surface of PPE-2 at the synthesis temperature of 140 °C (FM140). With a further increase in the synthesis temperature to 160 °C, the cube-like nanorods of Fe_3O_4 were formed in the FM160 sample. At the final synthesis temperature of 180 °C, rod-shaped nanocrystals were aggregated in the FM180 sample. Also, the sizes and morphologies of Fe_3O_4 nanocrystals formed on the surface of PPE-2 varied: 200–400 nm for nanospheres in FM140, 50–200 nm for nanocubes in FM160, and 5–25 nm for nanorods in FM180. The SEM results confirm that Fe_3O_4 nanocrystals with different sizes and morphologies can be synthesized on the surface of PPE-2 by simply changing the synthesis temperature and time.

From the energy-dispersive X-ray spectroscopy (EDS) spectrum of the FM180 sample in Fig. 4, the presence of C, Cl, N, O, and Fe elements can be confirmed. The EDS spectrum also shows the distribution of elements on the cross-sectional surface of magnetic Fe_3O_4/PPE-2 functional material. The EDS element mapping images in Fig. 5 show that the detected elements are uniformly distributed on the surface of PPE-2. This indicates the formation of Fe_3O_4 nanocrystals within the PPE-2 matrix by electrostatic and van der Waals effects between the functional groups of PPE-2 and Fe_3O_4 nanocrystals (Nguyen et al., 2021b).

Fig. 6 shows schematic illustration of the formation mechanism/stages of the Fe_3O_4/PPE-2 functional material. At the initial stage of the During the synthesis of Fe_3O_4/PPE-2 functional material, iron ions in the solution bind to amino groups in the PPE-2 anion exchanger through donor-acceptor bonds, van der Waals and electrostatic interactions. As a result, iron ions accumulate on the active surface of the PPE-2 anion exchanger. The system, which precipitated iron ions in the presence of

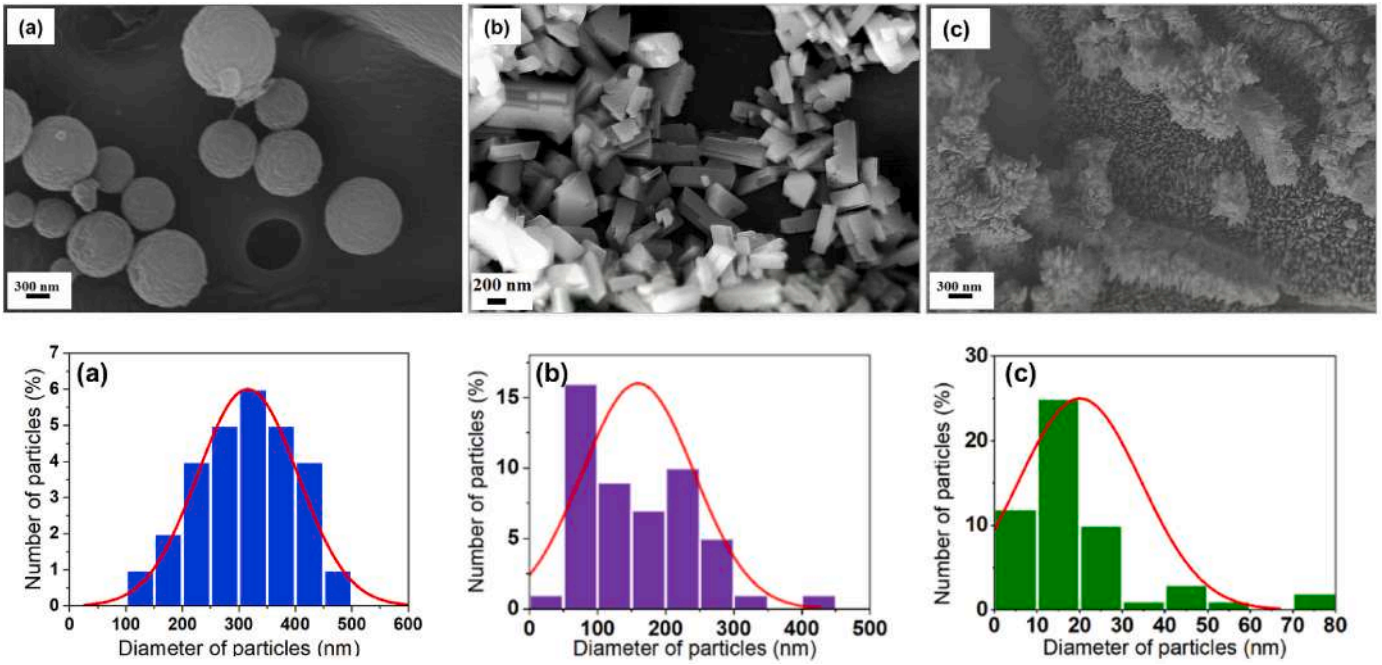

Fig. 3. SEM images of magnetic Fe_3O_4/PPE-2 functional material synthesized at different temperatures and times: (a) FM140, (b) FM160, and (c) FM180.

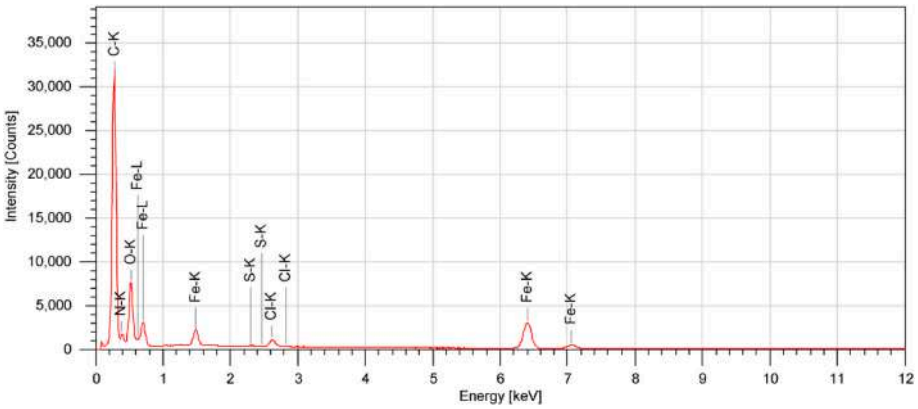

Fig. 4. EDS spectrum of magnetic Fe_3O_4/PPE-2 functional material (FM180).

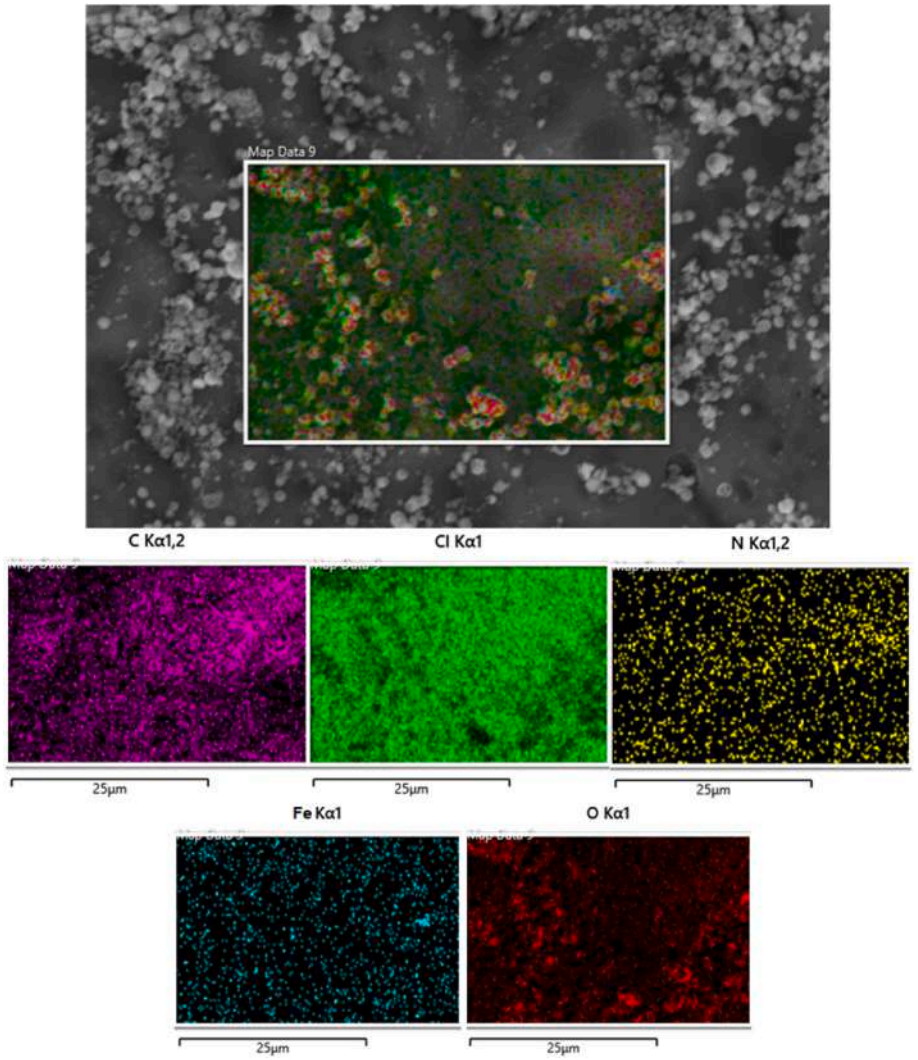

Fig. 5. EDS element mapping images of magnetic Fe_3O_4/PPE-2 functional material (FM180).

NH_4OH, was processed by hydrothermal method (Figure-6). When the hydrothermal synthesis process was carried out at a temperature of 140^0 C for 2 h (Figure-6a), spherical Fe_2O_3 crystals and partial Fe_3O_4 crystals were formed on the surface of the PPE-2 anion exchanger. When the temperature of the synthesis process was 160 °C and the duration was 4 h (Figure-6b), cubic Fe_3O_4 crystals formed on the surface of the PPE-2 anion exchanger. Addition, in the third stage, when the temperature and duration of the hydrothermal synthesis process was 180 °C and 6 h, a layer of nanorod-shaped Fe_3O_4 crystals was formed on the surface of the cubic crystals of FM160. Because of this, spherical Fe_3O_4 nanocrystals are formed at low temperatures, while nanocubic, nanorod, and nanostar Fe_3O_4 crystals are relatively difficult to form at high temperatures (Nguyen et al., 2021b). The formation of the Fe_3O_4/PPE-2 functional material involves a multi-step process, as